WILEY-VCH

Nitroxide-mediated polymerization of bio-based farnesene with a functionalized methacrylate

*Sharmaine B. Luk, Milan Marić**

S.B. Luk, Prof. M. Marić
Department of Chemical Engineering, McGill University, 3610 University Street #3060, Montreal, Quebec, H3A0C5, Canada
E-mail: milan.maric@mcgill.ca

Keywords: nitroxide-mediated polymerization, thermoplastic elastomers, alkoxyamine initiators, dienes, functional methacrylates

Farnesene is a bio-based terpene monomer that is similar in structure to commercially used dienes like butadiene and isoprene. Nitroxide-mediated polymerization (NMP) is adept for the polymerization of dienes, but not particularly effective at controlling the polymerization of methacrylates using commercial nitroxides. In this study, farnesene (Far) was statistically copolymerized with a functional methacrylate, glycidyl methacrylate (GMA), by NMP using *N*-succinimidyl modified commercial BlocBuilder® initiator (NHS-BB). Reactivity ratios were determined to be $r_{Far} = 0.54 \pm 0.04$ and $r_{GMA} = 0.24 \pm 0.02$. The ability of the poly(Far-*stat*-GMA) chains to re-initiate for chain extension with styrene showed a clear shift in molecular weight and monomodal distribution. Copolymerizations using a new alkoxyamine, Dispolreg 007 (D7), was explored as it was shown to homopolymerize methacrylates , but not yet reported for statistical copolymerizations. Bimodal molecular weight distributions were observed when an equimolar ratio of Far and GMA was copolymerized with D7 due to slow decomposition of the initiator, but chain-ends were active as shown by successful chain-extension with styrene. Both NHS-BB and D7 initiators were used to synthesize poly[Far-b-(GMA-*stat*-Far)] and poly(Far-*b*-GMA) diblock copolymers. While the NHS-BB initiated polymer chains had lower dispersity, D7 exhibited more linear polymerization kinetics and maintained more active chain-ends.

1. Introduction

Dienes (e.g. butadiene and isoprene) are industrially important monomers in making rubbery materials for applications like gasket and automotive parts, gloves and footwear, sealants, impact modifiers, and asphalt modifiers.[1-4] Poly(butadiene) and poly(isoprene) have low glass transition temperatures (T_g) of -100 and -70°C, respectively,[5] and are copolymerized with monomers or blended with thermoplastic resins based on styrene and/or acrylonitrile to impart viscoelastic properties to the material.[6-8] Styrene-butadiene rubber (SBR) and acrylonitrile-butadiene rubber (NBR) are typically synthesized industrially by emulsion conventional radical polymerization using redox catalysts or free radical initiators,[9, 10] but there are also cases of living/controlled radical polymerization (LRP/CRP) of SBR and NBR that provide polymers with controlled architectures.[11, 12] Styrene-butadiene (SBS) and styrene-isoprene (SIS) block copolymers have long been commercialized too, such as the Kraton™ family of thermoplastic elastomers, which are made by anionic polymerization.[13, 14]

While many industrial applications use free radical polymerization, controlled radical polymerization precisely controls the molecular architecture of polymer chains, therefore making homopolymers, diblock and triblock copolymers with narrow molecular weight distributions and low dispersity.[15] Ionic polymerization is a truly "living" method, but it is intolerant to functional monomers and impurities.[16] Controlled radical polymerization, more properly defined as reversible deactivation radical polymerization (RDRP), is a newer, more versatile technique in controlling the polymerization of free radicals. It utilizes activation-deactivation equilibrium or reversible chain transfer to suppress irreversible termination such that the propagating radical is primarily in its dormant state.[17] Amongst the several types of RDRP, atom transfer radical polymerization (ATRP)[18-20] and reversible addition-fragmentation transfer (RAFT)[21-23] can

polymerize a wide variety of functional monomers like vinyl esters and (meth)acrylates. This study will focus on nitroxide-mediated polymerization (NMP) as it is particularly adept for polymerization of styrene-diene systems.[24-26]

NMP is able to polymerize functionalized styrene and acrylate monomers successfully,[27] however it is limited in its ability to maintain active-chain ends in the polymerization of methacrylates.[28, 29] It was discovered that the rate of dissociation (k_d) is very large because of steric stabilization of the propagating methacrylate radical, and the rate of combination (k_c) is very low due to steric hindrance provided by the bulky SG1-nitroxide (*N*-*tert*-butyl-*N*-[1-diethylphosphono-(2,2-dimethylpropyl)] nitroxide). Consequently, the activation-deactivation equilibrium ($K_{eq} = k_d/k_c$) is high, resulting in termination by disproportionation.[30] To overcome this, small amounts of controlling comonomer like styrene or acrylonitrile can be added to effectively lower K_{eq}.[28, 31] Furthermore, the SG1-based nitroxide, BlocBuilder®, can be modified with an *N*-succinimidyl ester group (NHS-BB) to better control the polymerization of methacrylates,[32] and successful polymerization of various methacrylates was done using SG1-nitroxides with 5-10 mol% of styrene.[33-35]

Several alternative initiators have been investigated for the homopolymerization of methacrylates as well. 2,2-Diphenyl-3-phenylimino-2,3-dihydroindol-1-yloxyl nitroxide (DPAIO) based alkoxyamine was able to homopolymerize methyl methacrylate (MMA) to high conversion with low dispersity, but was not able to polymerize acrylates or styrene in ensuing chain-extensions.[36] An *N*-phenylalkoxyamine initiator (*N*-(1-methyl-(1-(4-nitrophenoxy)carbonyl) ethoxy)-*N*-(1-methyl-(1-(4-nitrophenoxy)carbonyl)ethyl)benzenamine) was also able to homopolymerize MMA but only to low conversion (X<50%).[37] More recently, a new class of alkoxyamines was developed that is able to homopolymerize methacrylates without

using controlling comonomer in solution and miniemulsion polymerization.[38-40] This new alkoxyamine, 3-(((2-cyanopropan-2-yl)oxy)(cyclohexyl)amino)-2,2-dimethyl-3-phenylpropanenitrile, which the authors have named Dispolreg 007 (D7), has a higher k_c, therefore exhibiting better control of the polymerization of methacrylates with minimal irreversible termination and successful chain-extension with n-butyl acrylate.

It is advantageous to incorporate methacrylates into poly(diene) materials because methacrylates can have a broad range of T_gs – e.g. poly(isobornyl methacrylate) has T_g ~190ºC[41] and poly(glycidyl methacrylate) has a T_g of 80°C, while poly(butyl methacrylate) has T_g = 20ºC.[42] Additionally, many methacrylates possess functional groups which can be incorporated into such hybrid materials. For example, they can act as compatibilizers for polymer blending. Glycidyl methacrylate (GMA) has been used to functionalize polymers (either by peroxide grafting or by *a priori* copolymerization) which can then be used to compatibilize immiscible polymer blends by grafting or reactive extrusion, where the epoxy group of GMA reacts with the carboxyl or hydroxyl groups of the immiscible polymer to form an *in situ* copolymer prevent phase separation.[43-45]

Moreover, there is increasing interest in replacing petroleum-derived monomers with renewable sources. Terpene-based monomers such as myrcene and farnesene have emerged as one possible source providing an alternative to traditionally petroleum-derived butadiene and isoprene monomers **(Schematic 1)**. Myrcene and farnesene are both found in nature, but can also be produced by pyrolysis of β-pinene[46] and microbial pathways from glucose,[47] respectively. Although, there are new bio-based pathways to synthesize butadiene and isoprene, [48-50] myrcene and farnesene are made up of multiple isoprene units, which can provide different rheological properties. It was shown that bottlebrush polymers with densely packed, long side-chains improve elastic properties. [51, 52] Furthermore, myrcene and farnesene are non-volatile compounds so they

can be polymerized in atmospheric conditions without using pressurized vessels as would be necessary for isoprene or butadiene.

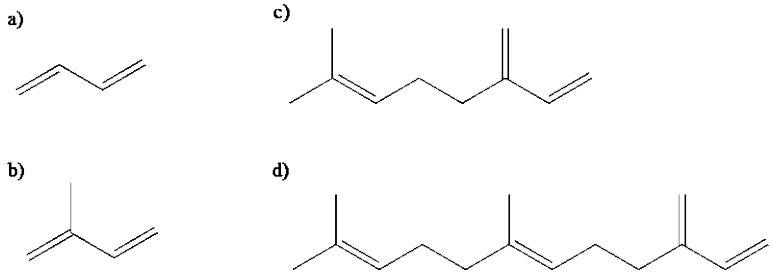

Schematic 1. Chemical structures of a) 1,3-butadiene, b) isoprene, c) myrcene, and d) farnesene.

Myrcene has been copolymerized with monomers typically used for thermoplastics like α-methyl-*p*-methylstyrene[53] and poly(lactic acid)[54] by anionic polymerization, and more recently copolymerized with GMA and styrene by NMP.[55, 56] Farnesene has been homopolymerized by ionic polymerization,[57] but polymerization by RDRP has not yet been reported. This study investigates nitroxide-mediated polymerization of bio-based farnesene with incorporation of functional GMA. The homopolymerization of farnesene (Far) and copolymerization with GMA using NHS-BB were done to determine reactivity ratios and hence expected microstructure. The ability of the D7 to control the copolymerization of Far and GMA was also examined, and the kinetics were thoroughly discussed and contrasted with SG1-nitroxides. Poly(Far-*b*-GMA) diblock copolymers were made using both NHS-BB and D7, and discussions regarding the important parameters governing microstructural control (eg. molecular weight versus conversion, dispersity, and chain-end fidelity) were compared.

2. Experimental Section

2.1. Materials

Trans-β-farnesene, known as Biofene® (Far, ≥95%) was obtained from Amyris. Glycidyl methacrylate (GMA, 97%) and styrene (St, ≥99%) monomers were purchased from Millipore Sigma. Monomers were purified using 1.0 g of aluminum oxide (basic Al_2O_3, activated,

Brockmann I) and 0.05 g calcium hydride (CaH_2, ≥90%) per 50 mL of monomer, which were used as purchased from Millipore Sigma. 2-([*tert*-Butyl[1-(diethoxy-phosphoryl)-2,2-dimethylpropyl]amino]oxy)-2-methylpropionic acid or BlocBuilder® was purchased from Arkema and modified with an *N*-succinimidyl ester group following a method used in literature to synthesize 2-methyl-2-[*N*-*tert*-butyl-*N*-(1-diethoxyphosphoryl-2,2-dimethylpropyl)-aminoxy]-*N*-propionyloxysuccinimide or NHS-BlocBuilder (NHS-BB).[58] 3-(((2-Cyanopropan-2-yl)oxy)(cyclohexyl)amino)-2,2-dimethyl-3-phenylpropanenitrile, Dispolreg 007, (D7) was synthesized according to the method described by Ballard *et al*.[38] Toluene (≥99%), methanol (MeOH, ≥99%), and tetrahydrofuran (THF, 99.9% HPLC grade) were obtained from Fisher Scientific and used as received. Deuterated chloroform ($CDCl_3$, 99.9% D) was purchased from Cambridge Isotope Laboratories, USA and used as received.

2.2. Methods

2.2.1. Synthesis of poly(Far-stat-GMA) copolymers

Statistical copolymers of Far and GMA were synthesized via nitroxide-mediated polymerization using NHS-BB and D7 initiators. Experiments for various molar ratios of Far and GMA were done in bulk and the amount of initiator was calculated based on a target molecular weight of 30,000 g mol^{-1}. See **Table S.1** for quantities of initiator and monomers for Far/GMA copolymerizations. Reaction mixtures were prepared in a 10 mL three-neck round-bottom flask, stirred, and bubbled with N_2 for 30 minutes. They were heated up to reaction temperature on a heating mantle with N_2 bubbling on top to ensure an oxygen-free environment with continuous stirring throughout the reaction. Samples were taken at various time points using a 1 mL syringe for conversion and molecular weight analysis. Polymers were purified by precipitation using methanol and dried in the vacuum oven at room temperature overnight.

2.2.2. Chain-extension of poly(Far-stat-GMA) macroinitiators

Several poly(Far-*stat*-GMA) macroinitiators were used for chain-extension: Far-rich and GMA-rich macroinitiators – both synthesized using NHS-BB, and equimolar poly(Far-*stat*-GMA) synthesized using D7. The syntheses of the macroinitiators were described previously for Far/GMA random copolymers. After purification, the macroinitiators were dissolved in toluene and 3:1 mass ratio of styrene to macroinitiator was added to the solution (50 wt% monomer in toluene). The reaction mixture was bubbled with N_2 for 30 minutes and remained under N_2 atmosphere throughout the reaction with stirring. The chain-extension reaction was done at 110°C and samples were taken at various time points using a 1 mL syringe for conversion and molecular weight analysis. The final polymer was precipitated again using methanol and dried in the vacuum oven at room temperature overnight.

2.2.3. *Synthesis of poly(Far-b-GMA) block copolymers*

Block copolymers were made by first synthesizing the Far homopolymer block using NHS-BB or D7 initiators in bulk at 120°C. The polymerization was typically stopped at a conversion of <50% to ensure high chain-end fidelity for chain-extension. The polymer was purified by precipitation in methanol and dried in a vacuum oven at room temperature overnight. The poly(Far) macroinitiator was dissolved in toluene and chain-extended with GMA or monomer mixture of 90 mol% GMA and 10 mol% Far (50 wt% monomer in toluene) at 110°C. Reaction mixtures were bubbled with N_2 for 30 minutes and remained under N_2 atmosphere throughout the reaction with stirring. Samples were taken using a 1 mL syringe for conversion and molecular weight analysis. The final polymer was precipitated again using methanol and dried in the vacuum oven at room temperature overnight.

2.2.4. *Polymer Characterization*

Overall monomer conversion was determined by proton nuclear magnetic resonance (^{1}H NMR, 16 scans) using a Varian/Agilent 500 MHz spectrometer. All NMR samples were prepared in deuterated chloroform ($CDCl_3$). Homopolymerization of Far was mostly by 1,4 addition with ~3 mol% of 1,2 addition as seen in **Figure S.1** in Supporting Information. The conversion of Far (X_{Far}) was calculated using **Equation 1** and A_δ is the area of proton peak integration. The Far monomer proton at δ = 6.4 ppm and the two singlets (three methyl groups, 9H) at δ = 1.65 ppm are used to determine X_{Far}. Conversion of GMA (X_{GMA}) was calculated using **Equation 2** using the two vinyl GMA monomer protons at δ = 6.2 and 5.6 ppm, and the peaks at δ = 4.4, 3.9, 2.8, 2.6 ppm, which include both monomer and polymer protons each. The overall conversion (X) for copolymerization of Far and GMA calculated using **Equation 3** is an average of the two monomer conversions based on the initial monomer compositions ($f_{Far,0}$ and $f_{GMA,0}$). See **Figure S.2** in Supporting Information for the NMR spectra of Far/GMA copolymerization.

$$X_{Far} = 1 - \frac{A_{6.4}}{\frac{A_{1.65}}{9}} \quad (1)$$

$$X_{GMA} = 1 - \frac{\frac{A_{6.2} + A_{5.6}}{2}}{\frac{A_{4.4} + A_{3.9} + A_{2.8} + A_{2.6}}{4}} \quad (2)$$

$$X = f_{Far,0}X_{Far} + f_{GMA,0}X_{GMA} \quad (3)$$

Monomer conversion of styrene (X_{St}) for chain-extension of poly(Far-*ran*-GMA) macroinitiators were determined by ^{1}H NMR as shown in **Figure S.3**. The vinyl protons of styrene are at δ = 5.3 and 5.8 ppm. For the conversion calculation, the vinyl proton at δ = 5.8 ppm is set to an normalized area of 1. Because the chain-extension reactions were done in toluene, the aromatic protons of toluene and styrene overlap in the δ = 7 – 7.5 ppm region and the polymer

protons are also in the range of δ = 6 – 7.5 ppm. Therefore, the singlet at δ = 2.4 ppm (toluene methyl group, 3H) is accounted for and subtracted from the total number of protons contributed by toluene and styrene (δ = 6.8 ppm, 1H) to determine the conversion as shown in **Equation 4**.

$$X_{St} = 1 - \frac{\frac{A_{5.8} + A_{5.3}}{2}}{\frac{\left(A_{6-7.6} - 1 - \frac{A_{2.4}}{3} \times 5\right)}{5}} \quad (4)$$

Number average molecular weight (M_n) and dispersity ($Đ = M_w/M_n$) of polymer samples were measured using gel permeation chromatography (GPC, Water Breeze) with HPLC grade tetrahydrofuran (THF) as an eluent at a flow rate of 0.3 mL min^{-1}. The GPC has three Waters Styragel HR columns (HR1 with a molecular weight measurement range of 10^2 to 5×10^3 g mol^{-1}, HR2 with a molecular weight measurement range of 5×10^2 to 2×10^4 g mol^{-1}, and HR4 with a molecular weight measurement range of 5×10^3 to 6×10^5 g mol^{-1}), a guard column, and a refractive index (RI 2414) detector. The columns were heated to 40°C during analysis. The molecular weights were determined relative to poly(methyl methacrylate) (PMMA) calibration standards from Varian Inc. (ranging from 875 to 1,677,000 g mol^{-1}). The reported molecular weights are all relative to the PMMA standards and not adjusted with Mark-Houwink parameters.

3. Results and Discussion

3.1. Statistical copolymerization of Far/GMA using NHS-BlocBuilder

The homopolymerization of methacrylates by NMP is generally done at 90-100°C due to the slow rate of recombination (k_c) between the nitroxide and methacrylate radical and fast propagation rate (k_p).[28, 29, 31] Lower temperature is ideal for limiting the formation of inactive chain-ends by irreversible termination. However, the homopolymerization of Far is much slower in comparison, and showed signs of chain-transfer below 120°C. The statistical copolymerizations of Far and GMA were all done at 120°C initially at 7 different monomer compositions ($f_{Far,0}$ = 0.1-

0.9) in bulk using NHS-BB. In GMA-rich compositions ($f_{Far,\,0}$ = 0.1 and 0.2), the conversion vs. time and the number average molecular weight (M_n) vs. conversion plots were not linear, and dispersity was high (Đ>1.6) as shown in **Figure S.4** and **Figure S.5**. This indicated the polymerizations were not well-controlled by the nitroxide, and polymer chains were not propagating after a certain conversion because the chain-ends were no longer active. The increase in dispersity was further indication that the chains have irreversibly terminated.

The GMA-rich copolymerizations were repeated at 90°C, and were much more controlled than at 120°C. As seen in **Figure 1a**, the conversion vs. time plots for the GMA-rich copolymerizations at 90°C show a linear correlation with reaction time. The GMA-rich polymerizations at high conversion (~80%) became very viscous and accelerated the reaction, therefore the last conversion data did not follow the linear trend and was not included in **Figure 1a**. However, the Mn vs. Conversion plots in **Figure 2a** including the high conversion data points were linear. The more Far-rich copolymerizations done at 120°C are shown in **Figure 1b** and also show linear correlations. The linearity of these copolymerizations show that the majority of the polymer chains remained active throughout the reaction even to higher conversions, as the solid trend line was extended to the end of the reactions.

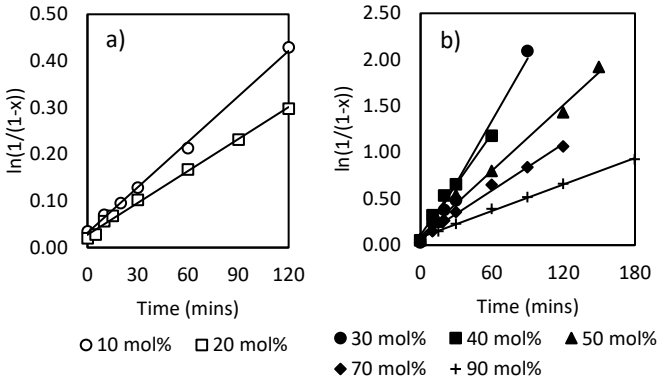

Figure 1. Linearized conversion as a function of reaction time for the random copolymerizations of Far/GMA at various Far compositions at a) 90 and b) 120°C in bulk using NHS-BB.

Molecular weight of the Far/GMA copolymerizations increased linearly with conversion as well, as shown in **Figure 2**. ~~At 90°C, the experimental M_n was slightly above the theoretical M_n, which could be due to reduced initiator efficiency at a lower temperature.~~ The fast increase in Đ in **Figure 3a** suggests low initiator efficiency as the initial high Đ means not all chains were initiated at the same time. The final dispersity at $f_{far,0}$ = 0.1 and 90°C in **Figure 3a** was quite high (~1.8) likely due to the high viscosity at the end of the reaction leading to irreversible termination. At 120°C, the M_n values were all very close to the theoretical M_n values with the exception for $f_{Far,\,0}$ = 0.3, where the growth of polymer chains slightly deviated from linearity. However, looking at the Đ values in **Figure 3b**, the highest Đ was ~1.5. Linear increase in molecular weight and low Đ suggest that most chains have active chain-ends and are growing simultaneously at a controlled rate.

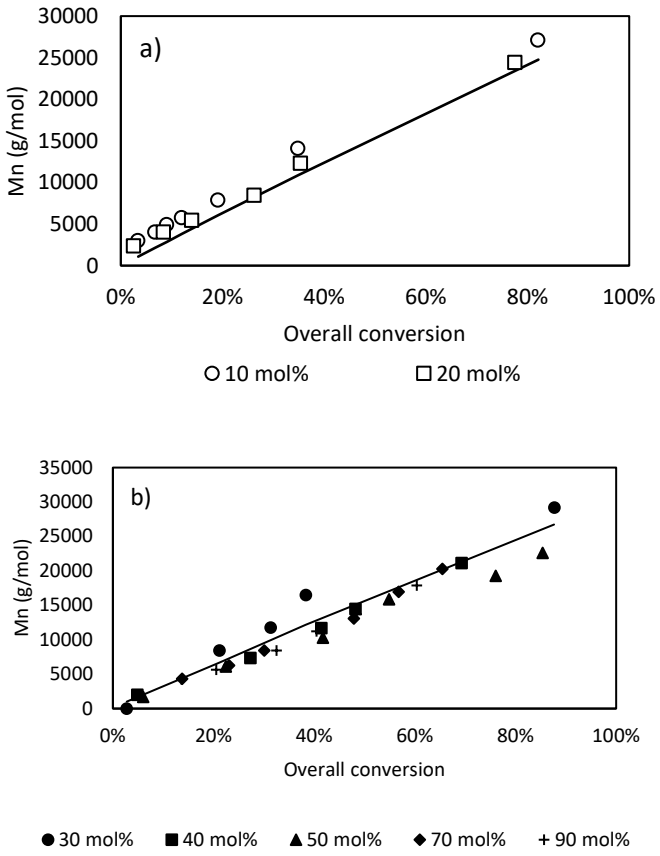

Figure 2. Number averaged molecular weight (M_n) as a function of conversion for random copolymerizations of Far/GMA at various Far compositions at a) 90 and b) 120°C in bulk using NHS-BB. The solid lines represent the theoretical molecular weight calculated from the conversion based on a target molecular weight of 30,000 g mol^{-1}.

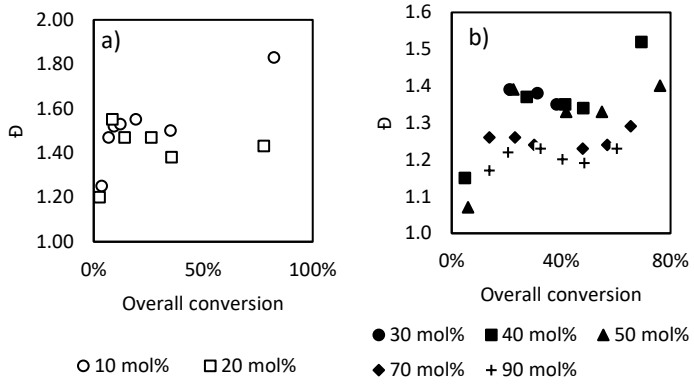

Figure 3. Dispersity (Đ) as a function of overall conversion for random copolymerization of Far/GMA at various Far compositions in bulk at a) 90 and b) 120°C using NHS-BB.

A limitation of NMP is that the homopolymerization of methacrylates using SG1-based initiators requires 5-10 mol% of controlling comonomer to maintain high chain-end fidelity.[32, 34, 35, 59] Styrene is most commonly used as a controlling comonomer because it effectively lowers the activation-deactivation equilibrium (<*K*>) of the nitroxide by penultimate effects.[60] In these statistical Far/GMA copolymerizations, it seems that Far can act as a controlling comonomer for the homopolymerization of GMA by adding 10 mol% of Far at 90°C, similar to isoprene when randomly copolymerized with methacrylates by NMP.[61] However, further decreasing to 5 mol% farnesene, the Far/GMA copolymerization resulted in a high fraction of dead chains and high dispersity (~1.8).

The apparent rate constant of Far/GMA copolymerization by NMP is proportional to $<k_p><K>$, which is the product of the average propagation rate coefficient and average activation-deactivation equilibrium constant for Far and GMA. From the slopes of the linearized conversion vs. time plots in **Figure 1**, $<k_p><K>$ values can be determined from the theoretical expression for the activation-deactivation equilibrium expression shown in **Equation 5**, where C_0 is initial concentration of alkoxyamine initiator and $[N]_0$ is initial concentration of free nitroxide. [31]

$$\frac{d\left(\ln\left(\frac{1}{1-X}\right)\right)}{dt} = < k_p >< K > \frac{C_0}{[N]_0} \qquad (5)$$

The concentration of nitroxide can only be assumed to remain constant at low conversion, $[N]_0 = [N]$, because of possible irreversible termination of the nitroxide in the latter stages of the polymerization. Therefore, the $<k_p><K>$ values were calculated from the slope determined at X<60%. Furthermore, there was no excess free nitroxide added, so $C_0/[N]_0 = 1$. The $<k_p><K>$ values at different initial Far monomer fraction is shown in **Figure 4** and it is evident that the rate of Far/GMA copolymerization was slowed down by increasing Far content. The $<k_p><K>$ values

were also found to significantly decrease when isoprene and myrcene were copolymerized with methacrylates.[55, 61] Because $\langle k_p \rangle \langle K \rangle$ is a lumped term, the decrease in value can indicate a decrease in the averaged copolymerization propagation rate $\langle k_p \rangle$ and/or a decrease in the activation-deactivation equilibrium constant $\langle K \rangle$ depending on the terminal radical unit (Far or GMA).

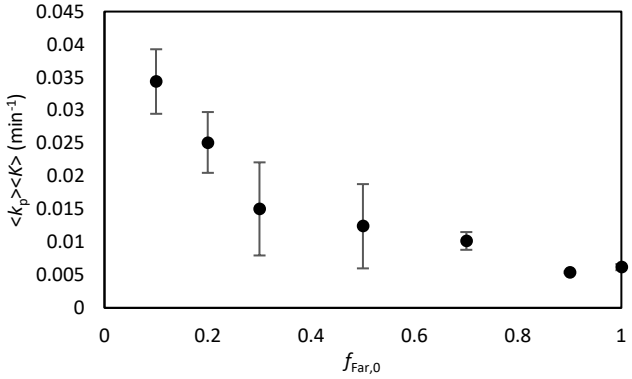

Figure 4. Average $\langle k_p \rangle \langle K \rangle$ as a function of initial Far monomer fraction for Far/GMA statistical copolymerizations using NHS-BB at 120°C in bulk. The error bars represent 95% confidence intervals.

3.2. Reactivity ratios of Far/GMA statistical copolymerization

Culminating all the statistical copolymerizations of Far and GMA at different monomer compositions at 120°C, a Mayo-Lewis plot was made as shown in **Figure 5**. The Mayo-Lewis equation **(Equation 6)** correlates instantaneous copolymer composition (F_i) as a function of comonomer feed composition (f_i) to infer the relative reactivity ratios (r_i) of species i.[62] This assumes the terminal model, meaning the reactivity of the propagating radical is only dependent on the terminal radical unit. If the reactivity ratios are at unity ($r_1 = r_2 = 1$), it indicates that the propagating radical is equally likely to add on the same monomer as the propagating radical (homopropagation) or the other monomer (cross-propagation).

$$F_1 = \frac{r_1 f_1^2 + f_1 f_2}{r_1 f_1^2 + 2 f_1 f_2 + r_2 f_2^2} \quad (6)$$

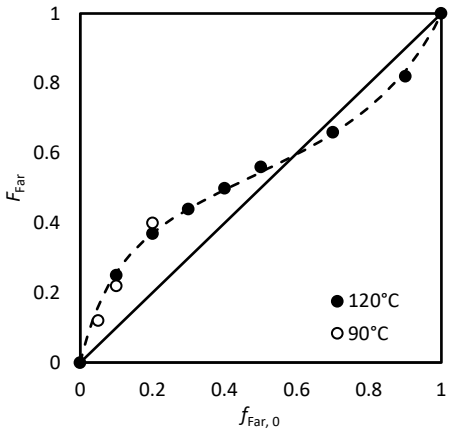

Figure 5. Mayo-Lewis plot for random copolymerization of farnesene and GMA in bulk at 120 and 90°C using NHS-BB. The dashed line is the Mayo-Lewis curve calculated using relative reactivity ratios r_{Far} = 0.54 and r_{GMA} = 0.24. The solid line represents the relative reactivity ratios at unity.

The relative reactivity ratios of Far/GMA copolymerization were estimated by fitting the F_{Far} vs. $f_{Far,0}$ data at 120°C using the Mayo-Lewis equation in MATLAB. The reactivity ratios were determined with 95% confidence intervals to be r_{Far} = 0.54 ± 0.04 and r_{GMA} = 0.24 ± 0.02. The cumulative polymer compositions were measured at low conversion (X<15%) (See **Table S.2**) to apply the Mayo-Lewis equation. Both reactivity ratios are <1, therefore both Far and GMA have higher cross-propagation rate coefficients than homopropagation. However, r_{Far} is about two times higher than r_{GMA}, so Far is slightly more preferentially incorporated into the copolymer. The Mayo-Lewis curve has an azeotrope at $f_{Far,0}$~0.62 and both ratios are <1, so the polymer composition is essentially random. Three data points from the 90°C experiments were included in the Mayo-Lewis plot as well. They were close to the estimated Mayo-Lewis curve determined at 120°C, which suggests that reactivity ratios were not greatly affected by temperature.

Other diene/GMA statistical copolymerizations like isoprene/GMA and myrcene/GMA have similar reactivity ratios estimated assuming the terminal model and are summarized in **Table 1**. Interestingly, as the terpene monomer side chains get longer, their reactivity ratios relative to

GMA increase. In other words, their homopropagation rate coefficients increase relative to cross-propagation. Myrcene/GMA have almost identical reactivity ratios, and isoprene is less reactive than GMA, whereas farnesene is more reactive than GMA. However, looking at the diene/MMA systems, dienes are consistently more reactive than MMA.

Table 1. Summary of reactivity ratios for butadiene (BD)/MMA, isoprene (IP)/MMA, myrcene (Myr)/MMA, IP/GMA, Myr/GMA, and Far/GMA copolymerizations

	r_{diene}	r_{MMA}
BD/MMA[63]	0.75 ± 0.05	0.25 ± 0.03
IP/MMA[64]	0.78 ± 0.13	0.4 ± 0.1
Myr/MMA[65]	0.44	0.27
	r_{diene}	r_{GMA}
IP/GMA[42]	0.119 ± 0.048	0.248 ± 0.161
Myr/GMA[55]	0.49 ± 0.13	0.50 ± 0.13
Far/GMA	0.54 ± 0.04	0.25 ± 0.02

In copolymerizations of St/GMA and St/MMA, it was concluded that GMA was more preferentially incorporated relative to alkyl methacrylates like MMA due to polarity of the epoxy ester.[66] The polar ester decreases electron density of the double bond, therefore increasing the incorporation of functional methacrylate, which was also observed in the copolymerization of St and 2-hydroxyethyl methacrylate (HEMA).[67] Nonetheless, all the diene/GMA systems have reactivity ratios <1, so these copolymers are random in composition which indicates the functionality in GMA is well-distributed throughout the polymer chain. The statistical copolymerization of Far/GMA using NHS-BB gave insight regarding composition of the polymer chains, chain-end moiety (Far in Far-rich compositions, and GMA in GMA-rich compositions), and would allow us to compare it to copolymerization with the new alkoxyamine (D7) later.

3.3. Chain-extension of poly(Far-*stat*-GMA) copolymers

To investigate whether the poly(Far-*stat*-GMA) copolymers made with NHS-BB have active chain-ends, they were chain-extended with styrene at 110°C in 50 wt% toluene. Two different macroinitiators were synthesized, GMA-rich and Far-rich, to compare the ability for the macroinitiators of different compositions to be re-initiated for polymerization. The compositions and properties of the macroinitiators are summarized in **Table 2**. The GMA-rich and Far-rich macroinitiators were synthesized with initial monomer fractions $f_{Far,0}$ = 0.2 and 0.8, respectively. After polymerization at X<60%, the actual polymer compositions were F_{Far} = 0.24 and 0.74, respectively.

Table 2. GMA- and Far-rich macroinitiators synthesized in bulk at 120°C using NHS-BB.

Macro-initiator	$f_{Far,0}$	$f_{GMA,0}$	X (%)	M_n (kg/mol)	Đ	F_{Far}	F_{GMA}
GMA-rich	0.2	0.8	58.2	23.0	1.63	0.24	0.76
Far-rich	0.8	0.2	56.9	19.2	1.33	0.74	0.26

The Đ of GMA-rich macroinitiator was fairly high (1.63), because it was synthesized at 120°C and polymerization of GMA is not as well-controlled at high temperatures. After 60 mins of chain-extension, the molecular weight did not increase very much in the next hour and the Đ increased to 1.77 as seen in **Table S.3**. The high Đ suggests a significant fraction of the polymer chains were terminated and could not continue to polymerize. This was expected as the GMA-rich macroinitiator started with a high Đ, with some of the chains already dead, but it was still able to chain-extend showing some pseudo-livingness.

The Far-rich macroinitiator had a lower Đ of 1.33, as anticipated, because Far-rich copolymerizations had much better control with the majority of the chains remaining active. The chain-extension reaction with styrene also increased linearly after 2 hours, while the Đ remained

low with a final Đ of 1.34 shown in **Table S.4**. Far-rich macroinitiators were mostly active and chain-extended successfully due to high chain-end fidelity.

The molecular weight distributions for the chain-extension reactions are shown in **Figure 6** and there was a clear shift/increase in molecular weight for both GMA- and Far-rich macroinitiators. Both sets of GPC traces showed a small low molecular weight tail, indicating some macroinitiator chains did not chain-extend. Nonetheless, both macroinitiators were re-initiated to a high level and continued to polymerize with styrene showing effective chain-extension with significant amount of active chain-ends.

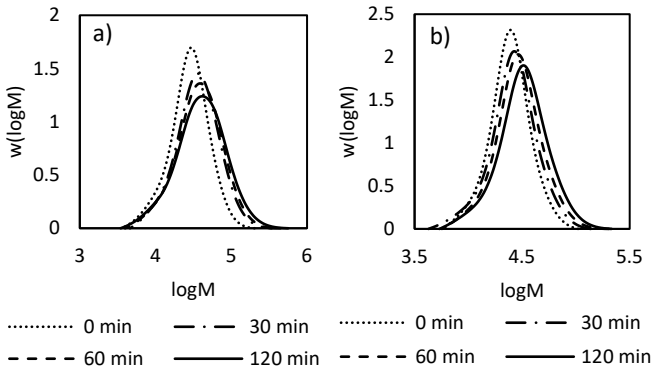

Figure 6. GPC traces of chain-extension reactions of a) GMA-rich and b) Far-rich macroinitiators with styrene in 50 wt% toluene at 110°C.

3.4. Statistical copolymerization of Far/GMA using Dispolreg 007

Nitroxide-mediated polymerization of methacrylates using conventional BlocBuilder or NHS-BlocBuilder is improved by adding a small portion of controlling comonomer,[29, 60] and recently a new class of alkoxyamines was developed via a readily scalable process that was able to homopolymerize methacrylates by NMP.[38-40] One alkoxyamine in particular, Dispolreg 007 (D7), showed good control over the polymerization of methyl methacrylate with a fast rate of polymerization, and can be easily synthesized from readily available reagents.[38] The chemical structures of the two initiators in this study are shown in **Schematic 2**. D7 has a higher k_c because

the steric hindrance provided by the *tert*-butyl and dimethyl groups on the nitroxide of NHS-BB is replaced with the cyclohexyl and benzyl groups on D7. This new alkoxyamine has not yet been reported for the copolymerization of methacrylates with other types of monomers, therefore it was directly applied to this study for the copolymerization of Far and GMA.

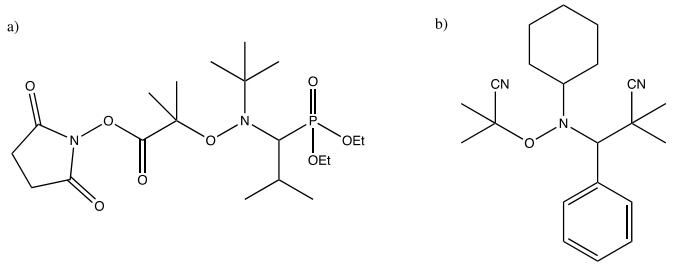

Schematic 2. Chemical structures of a) NHS-modified BlocBuilder (NHS-BB) and b) D7 alkoxyamine.

Copolymerization of equimolar Far and GMA was done using D7 as the alkoxyamine initiator in bulk at 120 and 90°C. The GPC traces of the copolymers synthesized using D7 at both temperatures showed a hint of a shoulder in the molecular weight distribution (MWD) **(Figure 7)**, and increased the Đ as a result **(Figure 8)**. Especially at 120°C, the Đ and M_n were initially high, indicating slow decomposition of the alkoxyamine, which is consistent with literature.[38-40] As the polymerization progressed, new chains continue to be initiated slowly until the chain lengths approached the theoretical M_n and consequently Đ decreased.[68] In previous studies, the slow decomposition was suppressed by increasing the temperature, however, the dispersity at 120°C was higher than at 90°C. It is likely that the temperature was too high at 120°C for the polymerization to remain well-controlled, creating more dead chains.

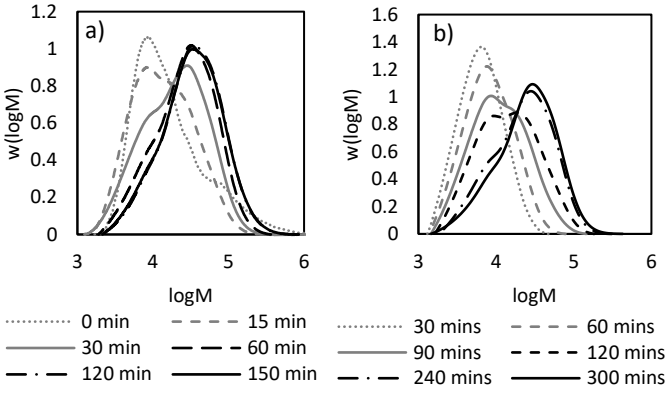

Figure 7. GPC traces of 50/50 molar ratio of Far/GMA random copolymerizations in bulk using D7 at a) 120 and b) 90°C.

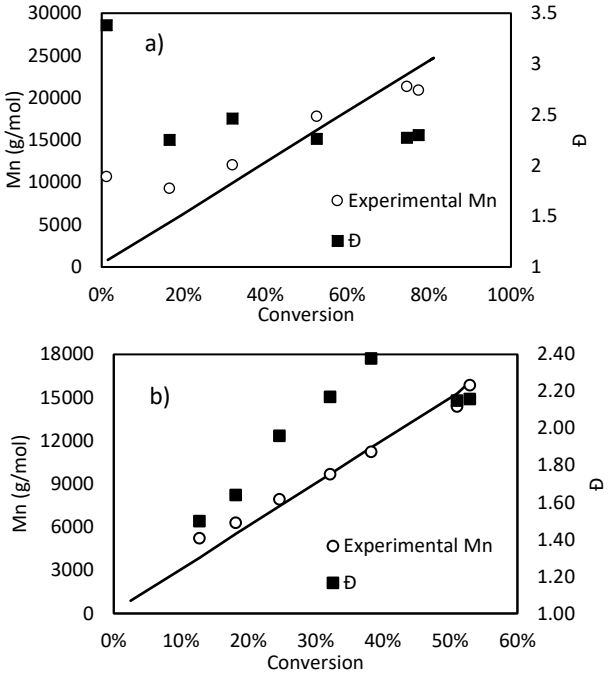

Figure 8. Number average molecular weights (Mn) and dispersity (Đ) plotted as a function of conversion for 50/50 molar ratio of Far/GMA random copolymerizations with D7 in bulk at a) 120 and b) 90°C. The solid line is the theoretical M_n calculated from the conversion based on a target molecular weight of 30,000 g mol^{-1}.

Despite the slow decomposition, homopolymerization of methyl methacrylate and n-butyl methacrylate using D7 did not result in a shoulder in the MWD, only increasing the Đ.[39, 40] Furthermore, irreversible termination of chains in copolymerizations of Far and GMA using NHS-BB in GMA-rich compositions broadened the molecular weight distribution and created a low

molecular weight tail, but not a shoulder. The Far/GMA copolymers synthesized using D7 had more of a shoulder at 90°C than at 120°C, so the apparent shoulder in the MWD is not due to irreversible termination, which should be more prominent at higher temperatures. The shoulder in the MWD (or bimodal distribution) suggests there are two populations of polymer chains that are distinctly different in chain length, which was not seen in homopolymerizations using D7 or copolymerizations using NHS-BB.

In **Figure 9**, the MWD for 50/50 Far/GMA copolymer is overlaid with the MWDs of Far and GMA homopolymers all synthesized using D7 at 90°C. The shoulder of the copolymer matches the peak of the Far homopolymer, and the taller peak of the copolymer matches the peak of the GMA homopolymer. This seems to suggest that the two populations of polymer chains are different in length and in composition, where the shorter chains are Far-rich and the longer chains are GMA-rich.

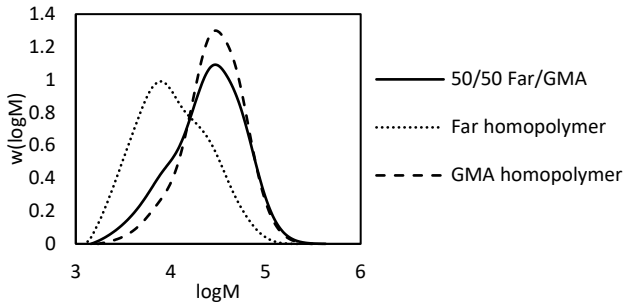

Figure 9. GPC traces of 50/50 molar ratio of Far/GMA random copolymer, farnesene homopolymer, and GMA homopolymer at 90°C in bulk using D7.

In a study investigating nitroxide-mediated copolymerization, copolymer composition was found to deviate from the terminal model largely due to asymmetry of the copolymerization parameters. This is especially evident before the activation-deactivation equilibrium (quasi-equilibrium condition or QEC) is established. [69] The rate at which the QEC is established relative

to cross-propagation is important to consider in all types of RDRP including ATRP[70, 71] and RAFT polymerization.[72]

The Far and GMA reactivity ratios obtained earlier, using NHS-BB initiator and assuming a terminal model, were $r_{Far} = 0.54$ and $r_{GMA} = 0.24$, which means the cross-propagation coefficients are two and four times higher than the homopropagation coefficients for Far and GMA, respectively. Furthermore, the rate of decomposition for D7 ($k_{d,90C} = 0.001$ s^{-1}) is much slower than BlocBuilder ($k_{d,90C} = 0.046$ s^{-1}).[38] The slow rate of decomposition limits the source of radicals, which delays the rate at which QEC is established. Before QEC is established, the radical populations are predetermined by the cross-propagation kinetics.[69] Because D7 has a slow rate of decomposition and both Far and GMA tend to cross-propagate, these Far/GMA copolymers synthesized using D7 do not have good chain-to-chain compositional homogeneity.

The averaged propagation rate coefficient for isoprene and GMA copolymerization was slowed down significantly compared to the homopolymerization of GMA by free radical polymerization ($k_p^{cop} = 42$ L mol^{-1} s^{-1} at $f_{GMA,0} = 0.24$ vs. $k_{p,GMA} = 600$ L mol^{-1} s^{-1} at 25°C).[73] Propagation coefficients were not obtained for Far/GMA, but as seen previously the $<k_p><K>$ values decreased significantly by increasing Far monomer composition. This suggests that the homopropagation of Far is much slower than GMA, and Far is slightly more prone to homopropagation than GMA according to their reactivity ratios.

Therefore, several factors can be used to rationalize the bimodal distribution of the Far/GMA copolymers with D7. Far monomers were initiated, and when they did homopropagate, they grew very slowly into short, Far-rich chains. GMA monomers were also initiated, and although they did not homopropagate as much, the homopropagation was very fast and grew into long, GMA-rich chains. Both of these populations were established pre-QEC, and continued to

polymerize in a controlled fashion once the nitroxide population has stabilized. The bimodal distribution could also be due to a difference in initiation rate for Far and GMA monomers and/or a large difference in equilibrium constants for Far and GMA propagating radicals (K_{Far} and K_{GMA}). However, further kinetic studies will need to be done to verify these justifications.

Nonetheless, poly(Far-*stat*-GMA) copolymer made with D7 was successfully chain-extended with styrene at 110°C in 50 wt% toluene. This further indicates the shorter chains were not formed due to irreversible termination, because they were re-initiated and continued to polymerize with styrene. In fact, the dispersity decreased from 2.07 initially to 1.80 after three hours, as M_n increased from 19 to 30 kg mol^{-1}. It is evident from the GPC traces in **Figure 10** that the shoulder eventually disappeared, and the Đ became lower.

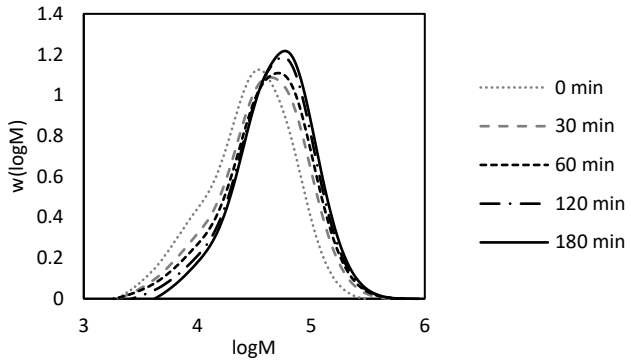

Figure 10. GPC traces for chain-extension of 50/50 molar ratio of Far/GMA macroinitiator using D7 with styrene in 50 wt% toluene at 110°C

3.5. Block copolymers using NHS-BlocBuilder vs. D7

CRP is well-known to tightly control chain-to-chain composition and molecular structure of polymer chains. Styrene-*b*-acrylic acid (PS-*b*-PAA) block copolymers were made by NMP with precisely controlled dispersity and block lengths to use as stabilizers in emulsion polymerization.[74] Although it was also shown that these surfactants do not require low dispersity to create a stable emulsions.[75] Therefore, the synthesis of Far-*b*-GMA diblock copolymers was

investigated using both NHS-BB and D7 initiators. First, the Far homopolymer block was synthesized using NHS-BB in bulk at 120°C, and the Far-NHS macroinitiator was used for two different chain-extension reactions with GMA. Another Far homopolymer macroinitiator was synthesized using D7 (Far-D7) in the same conditions for chain-extension with GMA. The properties of the two poly(Far) macroinitiators are summarized in **Table 3**. The homopolymerization of Far using NHS-BB was well-controlled as seen in **Figure S.6** resulting in a low Đ of 1.17. The homopolymerization of Far using D7 also showed linear chain growth with conversion as seen in **Figure S.7**, but is higher in Đ and molecular weight due to the slow initiation of D7.

Table 3. Summary of poly(Far) macroinitiators using NHS-BB and D7 synthesized in bulk at 120°C.

Macroinitiator	X (%)	M_n (g/mol)	Đ
Far-NHS	38	9100	1.17
Far-D7	45	18900	1.60

Far-NHS was first chain-extended with GMA without any controlling comonomer at 110°C in 50 wt% toluene. The polymerization rate was fast and molecular weight increased quickly after 90 minutes. When Far-NHS was chain-extended with GMA and 10 mol% Far (acting controlling comonomer), the final Đ is slightly lower than without Far, suggesting less irreversible termination. The dispersity of the Far-NHS chain-extensions with and without Far are 1.50 and 1.80 **(Table 4)**, respectively, so adding 10 mol% Far did aid in controlling the polymerization of GMA. The GPC traces for both chain-extensions of Far-NHS in **Figure 11** show that most chains were able to re-initiate and continued to polymerize throughout the reaction.

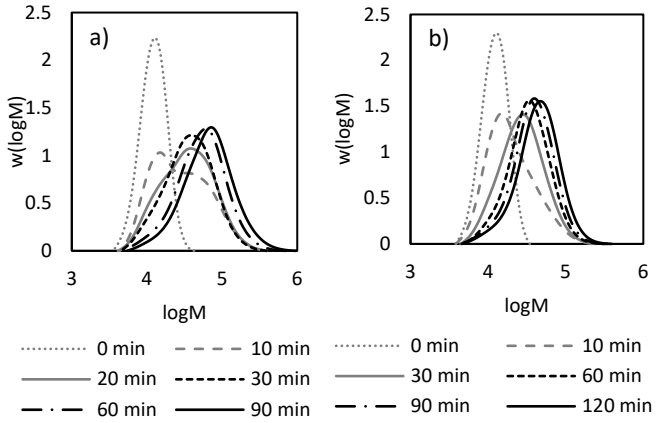

Figure 11. GPC traces of Far-NHS macroinitiator chain-extension with a) GMA and b) 10 mol% Far and 90 mol% GMA in 50 wt% toluene at 110°C.

A poly(Far) macroinitiator was synthesized with D7 initiator to examine whether it would also chain-extend with GMA. Similarly, it was done in 50 wt% toluene at 110°C. Looking at the GPC traces in **Figure 12**, the majority of the chains did chain-extend as seen by the shift in the MWDs. There is a more evident high molecular weight tail compared to the chain-extensions using Far-NHS macroinitiator resulting in a very high final Đ of 3.07 as seen in **Table 4**. The dispersity of Far-D7 was high to begin with because of the slow initiation of D7, however, it seems the re-initiation of Far-D7 macroinitiator is also slow therefore further increasing the dispersity.

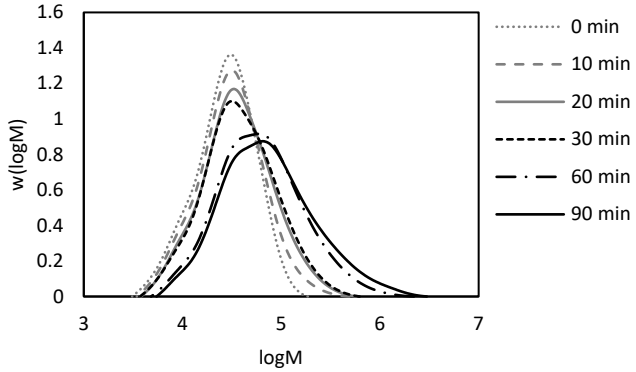

Figure 12. GPC traces of Far-D7 macroinitiator chain-extension with GMA in 50 wt% toluene at 90°C.

Table 4. Chain-extension of poly(Far) macroinitiators to make Far-*b*-GMA diblock copolymers. Cumulative polymer composition (F_{Far} and F_{GMA}) were determined by ^{1}H NMR.

Macroinitiator	$f_{Far,0}$	$f_{GMA,0}$	M_n (g/mol)	Đ	F_{Far}	F_{GMA}
Far-NHS	0	1	48100	1.80	0.38	0.62
Far-NHS	0.1	0.9	35100	1.50	0.63	0.37
Far-D7	0	1	44756	3.07	0.35	0.65

It may appear that chain-extension using D7 resulted in less active chain-ends because of the high final Đ compared to chain-extensions done with NHS-BB. However, looking at the increase of molecular weight with conversion in **Figure 13**, the chain-extensions of Far-NHS deviated more from linearity than chain-extension of Far-D7. With Far-NHS, molecular weight did not increase as linearly, indicating some degree of irreversible termination, whereas Far-D7 increased linearly in molecular weight meaning most of the chains continued to polymerize.

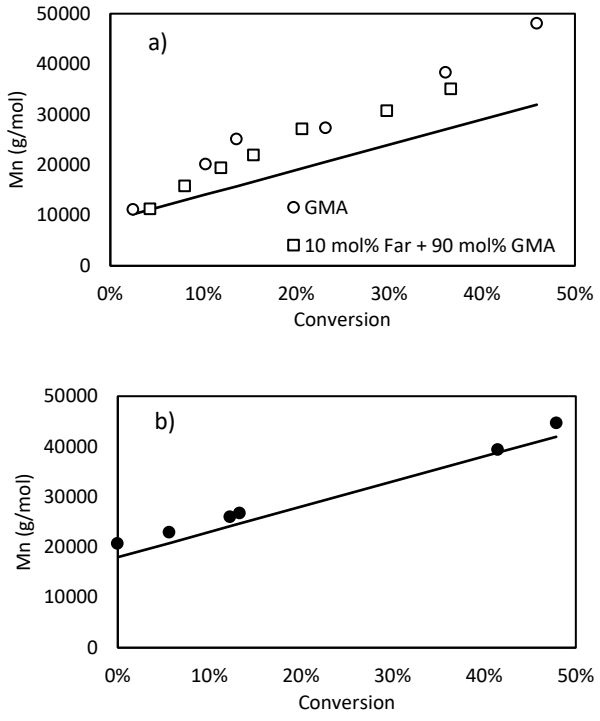

Figure 13. Molecular weight (M_n) and dispersity (Đ) vs. conversion plots for chain-extension of a) Far-NHS with GMA with and without 10 mol% Far, and b) chain-extension of Far-D7 with GMA at 110°C and 50 wt% toluene.

The new alkoxyamine, D7, was designed to better control the polymerization of methacrylates. In the chain-extension of Far-D7, it did exhibit better control over the polymerization of GMA as most chain-ends remained active. The chain-extensions done with NHS-BB was not as well-controlled and adding 10 mol% of Far improved the chain-extension with GMA slightly. The diblock Far-*b*-GMA copolymers made with D7 vary greatly in chain length for the respective Far and GMA blocks as shown by the high Đ. However, the polymer chains have distinct homogeneous blocks of Far and GMA while maintaining active chain-ends for perhaps another chain-extension, which is an advantage over NHS-BB.

4. Conclusion

The bio-based monomer, farnesene, was successfully statistically copolymerized with epoxy-functional GMA by nitroxide-mediated polymerization. Although conventional SG1-based initiators are known to not control the polymerization of methacrylates well, statistical copolymerization of Far/GMA with NHS-BB showed that Far can act as a controlling comonomer at 10 mol% and 90°C. Furthermore, the low conversion data of Far/GMA copolymerizations were used to determine reactivity ratios (r_{Far} = 0.54 ± 0.04 and r_{GMA} = 0.24 ± 0.02) indicating the copolymers were essentially random in composition similar to isoprene/GMA and myrcene/GMA. The Far/GMA copolymers had active chain-ends as shown by successful chain-extension, although Far-rich macroinitiators exhibited better control than GMA-rich macroinitiators.

The statistical copolymerization using NHS-BB provided a good basis for assessment of the new alkoxyamine, D7, which was shown to improve homopolymerization of methacrylates but not yet used in copolymerizations. The resulting Far/GMA copolymers synthesized with D7 had bimodal molecular weight distributions due to the slow decomposition of the initiator and asymmetry of the cross-propagation kinetics, which resulted in high dispersity but active chain-

ends. Synthesis of diblock poly(Far-*b*-GMA) and poly[Far-*b*-(GMA-*stat*-Far)] copolymers using NHS-BB and poly(Far-*b*-GMA) using D7 were compared. Chain-extension of Far-NHS with GMA was better controlled with 10 mol% Far added, but chain-extension of Far-D7 with only GMA had more active chain-ends. However, the slow initiation of D7 was still apparent in the chain-extension with GMA resulting in high dispersity. This study showed that Far can be polymerized by NMP for the first time, and copolymerization (statistical and block) with a functionalized GMA was done with both NHS-BB and D7, however, the copolymerization kinetics of the new alkoxyamine needs to be further investigated.

Supporting Information
Supporting Information is available from the Wiley Online Library or from the author.

Acknowledgements
The authors of this article would like to acknowledge Natural Sciences and Engineering Research Council of Canada (NSERC) Discovery (fund #288125), McGill Sustainability Systems Initiative New Ideas Fund, McGill University Faculty of Engineering, and McGill Engineering Doctoral Awards for the funding of this research. Also, the authors would like to thank the post-doctoral fellow, Adrien Metafiot, for useful scientific discussions while this research was being conducted.

Received: ((will be filled in by the editorial staff))
Revised: ((will be filled in by the editorial staff))
Published online: ((will be filled in by the editorial staff))

References

[1] J. G. Drobny, "15 - Applications of Thermoplastic Elastomers", in *Handbook of Thermoplastic Elastomers*, J.G. Drobny, Ed., William Andrew Publishing, Norwich, NY, 2007, p. 281.
[2] J. M. Degrange, M. Thomine, P. Kapsa, J. M. Pelletier, L. Chazeau, G. Vigier, G. Dudragne, L. Guerbé, *Wear* **2005**, *259*, 684.

[3] S. Wang, Q. Wang, X. Wu, Y. Zhang, *Construction and Building Materials* **2015**, *93*, 678.
[4] W. C. White, *Chemico-Biological Interactions* **2007**, *166*, 10.
[5] J. Brandrup, E. H. Immergut, E. A. Grulke, "*Polymer handbook"*, 4th ed. edition, Wiley, New York, 1999.
[6] M.-P. Bertin, G. Marin, J.-P. Montfort, *Polymer Engineering & Science* **1995**, *35*, 1394.
[7] I. Kopal, P. Koštial, Z. Jančíková, J. Valíček, M. Harničárová, P. Hybler, M. Kušnerová, "Modifications of Viscoelastic Properties of Natural Rubber/Styrene-Butadiene Rubber Blend by Electron Beam Irradiation", in *Improved Performance of Materials: Design and Experimental Approaches*, A. Öchsner and H. Altenbach, Eds., Springer International Publishing, Cham, 2018, p. 219.
[8] T. Masuda, A. Nakajima, M. Kitamura, Y. Aoki, N. Yamauchi, A. Yoshioka, "Viscoelastic properties of rubber-modified polymeric materials at elevated temperatures", in *Pure and Applied Chemistry*, 1984, p. 56/1457.
[9] T. O. Broadhead, A. E. Hamielec, J. F. MacGregor, *Die Makromolekulare Chemie* **1985**, *10*, 105.
[10] V. I. Rodríguez, D. A. Estenoz, L. M. Gugliotta, G. R. Meira, *International Journal of Polymeric Materials and Polymeric Biomaterials* **2002**, *51*, 511.
[11] M. Abbasian, H. Namazi, A. A. Entezami, *Polymers for Advanced Technologies* **2004**, *15*, 606.
[12] A. Kaiser, S. Brandau, M. Klimpel, C. Barner‐Kowollik, *Macromolecular Rapid Communications* **2010**, *31*, 1616.
[13] A. F. Johnson, D. J. Worsfold, *Journal of Polymer Science Part A: General Papers* **1965**, *3*, 449.
[14] U.S. US4219627A (1980), invs.: A. F. Halasa, J. E. Hall, A. Para;
[15] M. F. Cunningham, R. Hutchinson, "Industrial Applications and Processes", in *Handbook of Radical Polymerization*, John Wiley & Sons, Inc., 2003, p. 333.
[16] M. Szwarc, *Nature Nature* **1956**, *178*, 1168.
[17] D. Jenkins Aubrey, G. Jones Richard, G. Moad, "Terminology for reversible-deactivation radical polymerization previously called "controlled" radical or "living" radical polymerization (IUPAC Recommendations 2010)", in *Pure and Applied Chemistry*, 2009, p. 82/483.
[18] N. Chan, M. F. Cunningham, R. A. Hutchinson, *Macromolecular Chemistry and Physics* **2008**, *209*, 1797.
[19] M. Li, N. M. Jahed, K. Min, K. Matyjaszewski, *Macromolecules* **2004**, *37*, 2434.
[20] P. Raffa, M. C. A. Stuart, A. A. Broekhuis, F. Picchioni, *Journal of Colloid and Interface Science* **2014**, *428*, 152.
[21] S. Harrisson, X. Liu, J.-N. Ollagnier, O. Coutelier, J.-D. Marty, M. Destarac, *Polymers* **2014**, *6*, 1437.
[22] G. Moad, Y. K. Chong, A. Postma, E. Rizzardo, S. H. Thang, *Polymer* **2005**, *46*, 8458.
[23] K. Satoh, D.-H. Lee, K. Nagai, M. Kamigaito, *Macromolecular Rapid Communications* **2014**, *35*, 161.
[24] M. K. Georges, G. K. Hamer, N. A. Listigovers, *Macromolecules* **1998**, *31*, 9087.
[25] C. Detrembleur, V. Sciannamea, C. Koulic, M. Claes, M. Hoebeke, R. Jérôme, *Macromolecules* **2002**, *35*, 7214.
[26] J. K. Wegrzyn, T. Stephan, R. Lau, R. B. Grubbs, *Journal of Polymer Science Part A: Polymer Chemistry* **2005**, *43*, 2977.

[27] C. J. Hawker, A. W. Bosman, E. Harth, *Chemical Reviews* **2001**, *101*, 3661.
[28] Y. Guillaneuf, D. Gigmes, S. R. A. Marque, P. Tordo, D. Bertin, *Macromolecular Chemistry and Physics* **2006**, *207*, 1278.
[29] E. Guégain, Y. Guillaneuf, J. Nicolas, *Macromolecular Rapid Communications* **2015**, *36*, 1227.
[30] C. Dire, J. Belleney, J. Nicolas, D. Bertin, S. Magnet, B. Charleux, *Journal of Polymer Science Part A: Polymer Chemistry* **2008**, *46*, 6333.
[31] B. Charleux, J. Nicolas, O. Guerret, *Macromolecules* **2005**, *38*, 5485.
[32] A. Moayeri, B. Lessard, M. Maric, *Polymer Chemistry* **2011**, *2*, 2084.
[33] A. Darabi, P. G. Jessop, M. F. Cunningham, *Macromolecules* **2015**, *48*, 1952.
[34] B. Lessard, M. Marić, *Journal of Polymer Science Part A: Polymer Chemistry* **2009**, *47*, 2574.
[35] C. Zhang, B. Lessard, M. Maric, *Macromolecular Reaction Engineering* **2010**, *4*, 415.
[36] Y. Guillaneuf, D. Gigmes, S. R. A. Marque, P. Astolfi, L. Greci, P. Tordo, D. Bertin, *Macromolecules* **2007**, *40*, 3108.
[37] A. C. Greene, R. B. Grubbs, *Macromolecules* **2010**, *43*, 10320.
[38] N. Ballard, M. Aguirre, A. Simula, A. Agirre, J. R. Leiza, J. M. Asua, S. van Es, *ACS Macro Letters* **2016**, *5*, 1019.
[39] N. Ballard, M. Aguirre, A. Simula, J. R. Leiza, S. van Es, J. M. Asua, *Polymer Chemistry* **2017**, *8*, 1628.
[40] N. Ballard, A. Simula, M. Aguirre, J. R. Leiza, S. van Es, J. M. Asua, *Polymer Chemistry* **2016**, *7*, 6964.
[41] J. M. Yu, P. Dubois, R. Jérôme, *Macromolecules* **1996**, *29*, 7316.
[42] D. Contreras-López, E. Saldívar-Guerra, G. Luna-Bárcenas, *European Polymer Journal* **2013**, *49*, 1760.
[43] P. Juntuek, C. Ruksakulpiwat, P. Chumsamrong, Y. Ruksakulpiwat, *Journal of Applied Polymer Science* **2011**, *122*, 3152.
[44] Z. Su, Q. Li, Y. Liu, G.-H. Hu, C. Wu, *European Polymer Journal* **2009**, *45*, 2428.
[45] N. Zhang, Q. Wang, J. Ren, L. Wang, *Journal of Materials Science* **2009**, *44*, 250.
[46] A. Behr, L. Johnen, *ChemSusChem* **2009**, *2*, 1072.
[47] M. A. Rude, A. Schirmer, *Current Opinion in Microbiology* **2009**, *12*, 274.
[48] O. A. Abdelrahman, D. S. Park, K. P. Vinter, C. S. Spanjers, L. Ren, H. J. Cho, D. G. Vlachos, W. Fan, M. Tsapatsis, P. J. Dauenhauer, *ACS Sustainable Chemistry & Engineering* **2017**, *5*, 3732.
[49] O. A. Abdelrahman, D. S. Park, K. P. Vinter, C. S. Spanjers, L. Ren, H. J. Cho, K. Zhang, W. Fan, M. Tsapatsis, P. J. Dauenhauer, *ACS Catalysis* **2017**, *7*, 1428.
[50] M. D. Kumbhalkar, J. S. Buchanan, G. W. Huber, J. A. Dumesic, *ACS Catalysis* **2017**, *7*, 5248.
[51] S. J. Dalsin, M. A. Hillmyer, F. S. Bates, *Macromolecules* **2015**, *48*, 4680.
[52] W. F. M. Daniel, J. Burdyńska, M. Vatankhah-Varnoosfaderani, K. Matyjaszewski, J. Paturej, M. Rubinstein, A. V. Dobrynin, S. S. Sheiko, *Nature Materials* **2015**, *15*, 183.
[53] J. M. Bolton, M. A. Hillmyer, T. R. Hoye, *ACS Macro Letters* **2014**, *3*, 717.
[54] C. Zhou, Z. Wei, X. Lei, Y. Li, *RSC Advances* **2016**, *6*, 63508.
[55] A. Métafiot, J.-F. Gérard, B. Defoort, M. Marić, *Journal of Polymer Science Part A: Polymer Chemistry* **2018**, *56*, 860.

[56] A. Métafiot, Y. Kanawati, J.-F. Gérard, B. Defoort, M. Marić, *Macromolecules* **2017**, *50*, 3101.
[57] T. Yoo, S. K. Henning, *Rubber Chemistry and Technology* **2017**, *90*, 308.
[58] J. Vinas, N. Chagneux, D. Gigmes, T. Trimaille, A. Favier, D. Bertin, *Polymer* **2008**, *49*, 3639.
[59] A. Darabi, A. R. Shirin-Abadi, P. G. Jessop, M. F. Cunningham, *Macromolecules* **2015**, *48*, 72.
[60] J. Nicolas, C. Dire, L. Mueller, J. Belleney, B. Charleux, S. R. A. Marque, D. Bertin, S. Magnet, L. Couvreur, *Macromolecules* **2006**, *39*, 8274.
[61] D. Benoit, E. Harth, P. Fox, R. M. Waymouth, C. J. Hawker, *Macromolecules* **2000**, *33*, 363.
[62] F. R. Mayo, F. M. Lewis, *Journal of the American Chemical Society* **1944**, *66*, 1594.
[63] F. M. Lewis, C. Walling, W. Cummings, E. R. Briggs, W. J. Wenisch, *Journal of the American Chemical Society* **1948**, *70*, 1527.
[64] E. Oikawa, K. i. Yamamoto, *Polymer Journal* **1970**, *1*, 669.
[65] D. L. Trumbo, *Polymer Bulletin* **1993**, *31*, 629.
[66] W. Wang, R. A. Hutchinson, *Macromolecules* **2008**, *41*, 9011.
[67] K. Liang, M. Dossi, D. Moscatelli, R. A. Hutchinson, *Macromolecules* **2009**, *42*, 7736.
[68] F. Chauvin, P.-E. Dufils, D. Gigmes, Y. Guillaneuf, S. R. A. Marque, P. Tordo, D. Bertin, *Macromolecules* **2006**, *39*, 5238.
[69] I. Zapata-González, R. A. Hutchinson, K. Matyjaszewski, E. Saldívar-Guerra, J. Ortiz-Cisneros, *Macromolecular Theory and Simulations* **2014**, *23*, 245.
[70] B. Klumperman, G. Chambard, R. H. G. Brinkhuis, "Peculiarities in Atom Transfer Radical Copolymerization", in *Advances in Controlled/Living Radical Polymerization*, American Chemical Society, 2003, p. 180.
[71] K. Matyjaszewski, *Macromolecules* **2002**, *35*, 6773.
[72] A. Feldermann, A. Ah Toy, H. Phan, M. H. Stenzel, T. P. Davis, C. Barner-Kowollik, *Polymer* **2004**, *45*, 3997.
[73] F. Brandl, M. Drache, J. E. S. Schier, T. Nentwig, D. Contreras-López, E. Saldívar-Guerra, R. A. Hutchinson, S. Beuermann, *Macromolecular Rapid Communications* **2017**, *38*, 1700105.
[74] C. Burguière, S. Pascual, C. Bui, J.-P. Vairon, B. Charleux, K. A. Davis, K. Matyjaszewski, I. Bétremieux, *Macromolecules* **2001**, *34*, 4439.
[75] S. George, R. Champagne-Hartley, G. Deeter, D. Campbell, B. Reck, D. Urban, M. Cunningham, *Macromolecules* **2015**, *48*, 8913.